Graduate School in Biomedical Engineering and Medical Physics;
Transcranial Magnetic Stimulation (TMS)
4-8 August 2008
Helsinki University of Technology

INVERSE PROBLEM OF TMS-EVOKED EEG

Jukka Sarvas

Department of Biomedical Engineering and Computational Science,
Helsinki University of Technology

1 Preface and notation

This is a short introduction to the computing and the inverse problem of the TMS-evoked EEG potential. We only discuss the the EEG potential at a single moment of the time, but the results also apply to a time series of the EEG measurements if the possible time correlation of the sources is not taking into account. The emphasis is on the elementary field computing and the numerical simulation. Only the singular value truncation with the discrepancy principle and the L-curve method is introduced for treating the noisy data in the inversion problem.

In Chapter 2 we discuss the basic concepts of the EEG potential field and its computing and in Chapter 3 the related inverse problem in general. In Chapter 4 we treat the EEG potential of a layered sphere. In Chapters 5 and 6 the inverse problems of dipolar sources and sources distributed on surfaces are discussed. In Chapter 7 the regularization by the singular value truncation is introduced, and in Chapter 8 examples with synthetic data on the inversions of surface current sources in the layered sphere are presented.

In treating matrices we use the following MATLAB type *notation*. If A is an $M \times N$-matrix we denote by A^T its transpose, and by $A(m,:)$ its m:th row and by $A(:,n)$ its n:th column, $m = 1, \ldots, M,\ n = 1, \ldots, N$. The matrix A can also be presented by its columns as

$$A = [a_1, a_2, \ldots, a_N] \quad \text{with} \quad a_n = A(:,n), \tag{1.1}$$

or by its rows as

$$A = [b_1; b_2; \ldots; b_M] \quad \text{with} \quad b_m = A(m,:). \tag{1.2}$$

This notation also applies to vectors. A column vector is an $N \times 1$ matrix denoted as $a = [a_1; \ldots; a_N] = [a_1, \ldots, a_N]^T$, and a row vector is a $1 \times N$ matrix denoted as $b = [b_1, \ldots, b_N]$. The 3×1 column vectors we denote by bold-faced letters like $\mathbf{a}$.

2 Potential due to a current distribution in a conductive body

Le D be a conductive body in the 3-space with a possibly non-constant *conductivity* $\sigma(\mathbf{r}) > 0,\ \mathbf{r} \in D$. Outside D the conductivity $\sigma = 0$. Let $\mathbf{J}_p(\mathbf{r})$ be a *primary* (or source, impressed, driving) *current distribution* in the interior of D. Then the *electric potential* $V(\mathbf{r})$ due to $\mathbf{J}_p$ is the solution of the following (quasistatic and elliptic) *boundary value problem*,

$$\nabla \cdot (\sigma \nabla V) = \nabla \cdot \mathbf{J}_p \tag{2.1}$$

with the boundary condition

$$\frac{\partial V}{\partial n}(\mathbf{r}) = 0,\ \mathbf{r} \in S, \tag{2.2}$$

where the surface S is the boundary of D and

$$\frac{\partial V}{\partial n} = \widehat{\mathbf{n}} \cdot \nabla V$$

is the normal derivative of V on S with $\widehat{\mathbf{n}}$ being the (outer) unit normal of S. Here we assume that $\mathbf{J}_p$ does not flow out from D, i.e., $\mathbf{J}_p \cdot \widehat{\mathbf{n}} = 0$ on S. For a constant σ, (2.1) becomes the *Laplace's equation* $\nabla \cdot \nabla u = \nabla \cdot \mathbf{J}_p/\sigma$. With appropriate regularity demands on V the equation (2.1) with (2.2)

has a unique (weak) solution V up to an additive constant, for a rigorous formulation, e.g., see [1], page 197.

In our case D is the human head, $\mathbf{J}_p$ is the TMS-evoked (postsynaptic) current distribution in D, S is the surface of the scalp and $V(\mathbf{r})$, $\mathbf{r} \in S$, is the EEG potential, usually fixed by setting $V(\mathbf{r}_0) = 0$ on a reference point (electrode) $\mathbf{r}_0 \in S$.

In our case we also assume that σ is *piecewise constant*, which implies that $V(\mathbf{r})$ is the unique solution with the following properties: V is a continuous function everywhere in D, in each subdomain where σ is constant, V is twice continuously differentiable and on all interfaces T between two subdomains $D_j$and D_k with constant conductivities σ_j and σ_k, V satisfies the *interface condition*,

$$\sigma_j \frac{\partial V_j}{\partial n} - \mathbf{J}_{p,j} \cdot \widehat{\mathbf{n}} = \sigma_k \frac{\partial V_k}{\partial n} - \mathbf{J}_{p,k} \cdot \widehat{\mathbf{n}} \tag{2.3}$$

where V_j, V_k and $\mathbf{J}_{p,j}$, $\mathbf{J}_{p,k}$ are the potential and the primary current in D_j and D_k, respectively, and $\widehat{\mathbf{n}}$ is the unit normal of the interface. Furthermore, $\mathbf{E} = -\nabla V$ is the electric field, $\mathbf{J}_v = \sigma\mathbf{E} = -\sigma\nabla V$ is the *induced or volume current* and $\mathbf{J} = \mathbf{J}_p + \mathbf{J}_v$ is the *total current*. The equations (2.2) and (2.3) are the usual continuity conditions for the total current stating that the normal component of $\mathbf{J}$ must be continuous across any interface.

In the general case of a inhomogeneous (non-constant) conductivity σ usually the boundary value problem (2.1) - (2.2) is *numerically* solved by the *finite element method* (FEM). If σ is *piecewise constant*, and there are not too many subdomains of constant conductivity, the *boundary element method* (BEM) with the *surface integral equations* is also a practical numerical solving method for the problem (2.1) - (2.2).

In simple geometries like *a homogeneous full space* or a *homogeneous sphere*, an analytic solution for (2.1) - (2.2) is available, or a solution given by a series for some geometries like *a layered sphere*.

A *current dipole* with a *moment* $\mathbf{Q}$ at a point $\mathbf{r}'$ is the current element

$$\mathbf{J}_p(\mathbf{r}) = \delta(\mathbf{r} - \mathbf{r}')\,\mathbf{Q}, \tag{2.4}$$

where $\delta(\mathbf{r} - \mathbf{r}')$ is the Dirac's delta function. The potential $V(\mathbf{r})$ due to the current dipole $\mathbf{J}_p$ is given by

$$V(\mathbf{r}) = \mathbf{G}(\mathbf{r}, \mathbf{r}') \cdot \mathbf{Q}, \tag{2.5}$$

where $\mathbf{G}(\mathbf{r}, \mathbf{r}')$ is the *vector Green's function* of the potential problem (2.1) - (2.2); its components $G_j(\mathbf{r}, \mathbf{r}')$ are potentials due to the current dipoles

$$\mathbf{J}_k = \delta(\mathbf{r} - \mathbf{r}')\,\widehat{\mathbf{e}}_k,\ k = 1, 2, 3, \tag{2.6}$$

where $\widehat{\mathbf{e}}_1$, $\widehat{\mathbf{e}}_2$, $\widehat{\mathbf{e}}_3$ are the unit coordinate vectors $[1, 0, 0]^T$, $[0, 1, 0]^T$ and $[0, 0, 1]^T$ of the 3-space $\mathbb{R}^3$. We note that by the reciprocity of electric fields and sources, $\mathbf{G}(\mathbf{r}, \mathbf{r}')$ is equal to the electric field $\widetilde{\mathbf{E}}(\mathbf{r}')$ at $\mathbf{r}' \in D$ which we get by inserting unit electric current through electrodes at points $\mathbf{r}$ and $\mathbf{r}_0$ on S where $\mathbf{r}_0$ is the reference electrode (the sink).

If the Green's function of the potential problem is known, the potential due to a source current distribution $\mathbf{J}_p$ can be written as

$$V(\mathbf{r}) = \int_D \mathbf{G}(\mathbf{r}, \mathbf{r}') \cdot \mathbf{J}_p(\mathbf{r}')\, d^3r',\ \mathbf{r} \in D. \tag{2.7}$$

If the source $\mathbf{J}_p$ is distributed over a surface $T \subset D$ or on a line $L \subset D$, again the resulting potential is given by (2.7), where the integral is a surface integral over T or a line integral over L, respectively.

In a *homogeneous space* with a constant conductivity σ the potential V due to a current dipole $\mathbf{Q}$ at a point $\mathbf{r}'$ is given by

$$V(\mathbf{r}) = \frac{1}{4\pi\sigma} \frac{(\mathbf{r} - \mathbf{r}'}{|\mathbf{r} - \mathbf{r}'|} \cdot \mathbf{Q}, \tag{2.8}$$

and accordingly, the vector Green's function is as

$$\mathbf{G}(\mathbf{r}, \mathbf{r}') = \frac{1}{4\pi\sigma} \frac{(\mathbf{r} - \mathbf{r}')}{|\mathbf{r} - \mathbf{r}'|^3}. \tag{2.9}$$

So, the potential $V(\mathbf{r})$ due to a source current distribution $\mathbf{J}_p$ is by (2.7) as

$$V(\mathbf{r}) = \frac{1}{4\pi\sigma} \int \frac{(\mathbf{r} - \mathbf{r}')}{|\mathbf{r} - \mathbf{r}'|^3} \cdot \mathbf{J}_p(\mathbf{r}')\, d^3r' \tag{2.10}$$

$$= \frac{1}{4\pi\sigma} \int \frac{\nabla' \cdot \mathbf{J}_p(\mathbf{r}')}{|\mathbf{r} - \mathbf{r}'|}\, d^3r', \tag{2.11}$$

where the latter integral is obtained by using the identity:

$$\nabla' \cdot (\frac{1}{|\mathbf{r} - \mathbf{r}'|} \mathbf{J}_p(\mathbf{r}')) = \nabla'(\frac{1}{|\mathbf{r} - \mathbf{r}'|}) \cdot \mathbf{J}_p(\mathbf{r}') + \frac{1}{|\mathbf{r} - \mathbf{r}'|} \nabla' \cdot \mathbf{J}_p(\mathbf{r}')$$

and the Gauss divergence theorem.

3 Inverse problem

Let $V(\mathbf{r})$ be the potential in D due to the $\mathbf{J}_p$ as in (2.7). The EEG inverse problem is the following task: if the potential $V(\mathbf{r})$ is known on the outer surface S of D, find the source current $\mathbf{J}_p$. As well-known, in general, this inverse problem does not have a unique solution because of the existence of the so called *silent source currents* $\mathbf{J}_0$ in D which yield a zero potential on the surface S. Namely, such an current can always be added to the solution $\mathbf{J}_p$ of the inverse problem and $\mathbf{J}_p + \mathbf{J}_0$ is another solution because it yields the same surface potential on S. In the following some examples of silent currents are presented.

Obviously any primary current $\mathbf{J}_p$ in G with $\nabla \cdot \mathbf{J}_p = 0$ is silent due to (2.1). For instance, a closed current loop is a silent current of this type.

If T is a closed surface in some homogeneous subdomain of D and $\mathbf{J}_p$ is on T a uniform surface current directed normally to T, then $\mathbf{J}_p$ is silent, because in a homogeneous space the potential due to $\mathbf{J}_p$ is given by (2.10), which now becomes the double layer potential of a constant surface density and, therefore, vanishes outside T due to the solid angle theorem.

A rather general silent current $\mathbf{J}_p$ with $\nabla \cdot \mathbf{J}_p \neq 0$ is obtained by setting

$$\mathbf{J}_p = \sigma \nabla u$$

where u is a smooth function in some homogeneous subdomain W of D so that both $u = 0$ and $\frac{\partial u}{\partial n} = 0$ on the boundary of W. For instance, $u(\mathbf{r}) = 1 + cos(\pi \left|\mathbf{r}\right|^2)$, $|\mathbf{r}| \leq 1$, is such a function in the unit sphere. Outside W we set, $u = 0$. Then u satisfies (2.1) -(2.2), and therefore, the potential V due to $\mathbf{J}_p$ coincides with u, and it follows that $\mathbf{J}_p$ is silent. In addition, we easily can choose u so that $\nabla \cdot \mathbf{J}_p = \sigma \nabla \cdot \nabla u$ is non-vanishing.

Of course, there are plenty of *non-silent* primary currents. For instance, any finite set of current dipoles at different points forms a non-silent current source. A non-closed current curve with constant current strength is non-silent, as well as a finite set of them with separate end points.

An important example of non-silent currents is a *normally directed current distribution* $\mathbf{J}_p$ on a *non-closed surface patch*. In fact, such a current can be inverted uniquely from the (exact) surface potential if the patch is known.

This is important for EEG, because the cortical currents that produces the measured EEG are normally directed to the cortical surface.

Though the general EEG inverse problem does not have a unique solution, the situation greatly eases off, if we know that the primary current satisfies appropriate restrictions.

If we know that the source consists of finitely many current dipoles at different points, they can be, in principle, inverted from the (complete, non-noisy) surface potential.

If we know that the source is distributed on an open surface patch in D, the inverted source current, though not necessarily unique, may reveal some characteristic features of the true source, like roughly its spatial distribution.

4 EEG potential of a layered sphere

A layered sphere with spherical regions of constant conductivity is a simplified but widely used conductor model for the head. Besides its practical use in the EEG inverse analysis, it also is an instructive theoretical model for studying the realistic limits of the practical EEG inverse solution with noisy incomplete measurement data and the uncertainty caused by the non-uniqueness of the solution of the general EEG inverse problem.

Let us consider a layered sphere D with M spherical regions with constant conductivities $\sigma_1, \ldots, \sigma_M$ and the outer radii $r_1, \ldots, r_M$ so that the innermost region is the sphere $|\mathbf{r}| \leq r_1$ with the conductivity σ_1 and the j:th region is the shell $r_{j-1} \leq |\mathbf{r}| \leq r_j$ with the conductivity σ_j, $j = 2, \ldots, M$.

For the surface potential $V(\mathbf{r}),\ \mathbf{r} \in S$ due to a current dipole $\mathbf{Q}$ at a point $\mathbf{r}_Q,\ |\mathbf{r}_Q| \leq r_1$, we can for $V(\mathbf{r}) = V(\mathbf{r}, \mathbf{r}_Q, \mathbf{Q})$ derive an expression as the following series,

$$V(\mathbf{r}, \mathbf{r}_Q, \mathbf{Q}) = \frac{1}{4\pi\sigma_M} \sum_{n=1}^{\infty} \gamma_n \, r_Q^{n-1} \Big[\mathbf{Q} \cdot \widehat{\mathbf{r}}_Q \, n \, P_n(\widehat{\mathbf{r}} \cdot \widehat{\mathbf{r}}_Q) + (\widehat{\mathbf{Q}} \times \widehat{\mathbf{r}}_Q) \cdot (\widehat{\mathbf{r}} \times \widehat{\mathbf{r}}_Q) \, P_n'(\widehat{\mathbf{r}} \cdot \widehat{\mathbf{r}}_Q) \Big] \frac{1}{r^{n+1}} \tag{4.1}$$

where $\widehat{\mathbf{r}} = \mathbf{r}/r,\ r = |\mathbf{r}|,\ \widehat{\mathbf{r}}_Q = \mathbf{r}_Q/r_Q$ and $r_Q = |\mathbf{r}_Q|$, and the *translation*

coefficients γ_n are given by

$$\gamma_n = \frac{\frac{2n+1}{n+1}\, r_M^n}{\frac{n}{n+1}\, r_M^{2n+1}\, c_{1,1} - c_{2,1}} \tag{4.2}$$

where

$$\begin{bmatrix} c_{1,1} & c_{1,2} \\ \\ c_{2,1} & c_{2,2} \end{bmatrix} = C_{M-1} C_{M-2} \cdots C_1 \tag{4.3}$$

with the 2×2 matrices C_j given by

$$C_j = \frac{1}{2n+1} \begin{bmatrix} (n+1) + n\,\frac{\sigma_j}{\sigma_{j+1}} & (n+1)(1 - \frac{\sigma_j}{\sigma_{j+1}})\,\frac{1}{r_j^{2n+1}} \\ \\ n\,(1 - \frac{\sigma_j}{\sigma_{j+1}})\, r_j^{2n+1} & n + (n+1)\,\frac{\sigma_j}{\sigma_{j+1}} \end{bmatrix} \tag{4.4}$$

for $j = 1, \ldots, M-1$. If $M = 1$, we set $c_{1,1} = 1$ and $c_{2,1} = 0$ in (4.2) for all n. Furthermore, $P_n(t)$ is the Legendre polynomial of order n and $P_n'(t) = dP_n(t)/dt$ is its derivative, $n = 1, 2, \ldots$. Both $P_n(t)$ and $Q_n = P_n'(t)$ can easily be computed by the following algorithm:

$$P_0(t) = 1,\ P_1(t) = t,\ Q_0(t) = 0,\ Q_1(t) = 1, \tag{4.5}$$

and

$$P_{n+1}(t) = \frac{2n+1}{n+1}\, t\, P_n(t) - \frac{n}{n+1} P_{n-1}(t), \tag{4.6}$$

$$Q_{n+1}(t) = Q_{n-1}(t) + (2n+1) P_n(t), \tag{4.7}$$

for $n = 1, 2, \ldots$.

In (4.1) the series is written in terms of $P_n(t)$ and its derivative $P_n'(t)$, $n = 1, 2, \ldots$. In literature, e.g., see [2], usually this series is given in terms of $P_n(t)$ and the associated Legendre functions $P_n^1(t)$, $n = 1, 2, \ldots$; however, the latter form is not numerically stable if $\widehat{\mathbf{r}}_Q \times \widehat{\mathbf{r}} \approx 0$.

Note also that in (4.1) in forming $\widehat{\mathbf{r}}_Q = \mathbf{r}_Q / |\mathbf{r}_Q|$ we get division by zero if $r_Q = |\mathbf{r}_Q| = 0$. This can be avoided as follows: if $r_Q << 1$, say $r_Q < 10^{-8}\, r_1$, set

$$V(\mathbf{r}) = \frac{1}{4\pi\sigma_M}\, \gamma_1 \mathbf{Q} \cdot \widehat{\mathbf{r}}. \tag{4.8}$$

In a homogeneous sphere with the radius r and the constant conductivity $\sigma > 0$, $V(\mathbf{r}, \mathbf{r}_Q, \mathbf{Q})$ in (4.1) can also be given in an analytical form as

$$V(\mathbf{r}, \mathbf{r}_Q, \mathbf{Q}) = \frac{\mathbf{Q} \cdot \widehat{\mathbf{r}}_Q}{4\pi\sigma} \Big[\frac{2(\mathbf{r} \cdot \widehat{\mathbf{r}}_Q - r_Q)}{d^3} + \frac{1}{r_Q d} - \frac{1}{r\, r_Q} \Big] + \frac{(\mathbf{Q} \times \widehat{\mathbf{r}}_Q) \cdot (\widehat{\mathbf{r}} \times \widehat{\mathbf{r}}_Q)}{4\pi\sigma} \Big[\frac{2r}{d^3} + \frac{d + r}{r\, d\, (r + d - r_Q\, \widehat{\mathbf{r}} \cdot \widehat{\mathbf{r}}_Q)} \Big] \tag{4.9}$$

where $d = |\mathbf{r} - \mathbf{r}_Q|$, $\widehat{\mathbf{r}} = \mathbf{r}/r$, $\widehat{\mathbf{r}}_Q = \mathbf{r}_Q/r_Q$, $r = |\mathbf{r}|$ and $r_Q = |\mathbf{r}_Q|$. Again, if $r_Q << 1$, say $r_Q < 10^{-8}\, r$, then (4.8) with $\gamma_1 = 3/r^2$ yields

$$V(\mathbf{r}) = \frac{3\mathbf{r} \cdot \mathbf{Q}}{4\pi\sigma r^3}. \tag{4.10}$$

The layered sphere has often been used as an approximative conductor model of head in the EEG field analysis with three spherical regions: the *brain, skull* and *scalp*. Here we use in our numerical examples a head model with the radii

$$r_1 = 81\,\mathrm{mm},\ \mathrm{r}_2 = 85\,\mathrm{mm},\ \mathrm{r}_3 = 88\,\mathrm{mm}, \tag{4.11}$$

and conductivities

$$\sigma_1 = 0.33\ \Omega^{-1}\, m^{-1}, \quad \text{(brain)} \tag{4.12}$$

$$\sigma_2 = 0.0042\ \Omega^{-1}\, m^{-1}, \ \text{(skull)} \tag{4.13}$$

$$\sigma_3 = 0.33\ \Omega^{-1}\, m^{-1}, \quad \text{(scalp)}. \tag{4.14}$$

With (4.1) we have computed the EEG potential $V(\mathbf{r})$, $|\mathbf{r}| = r_3$, using $N = 50$ as the number of terms in the series (4.1). Also with (4.1) we can compute the vector Green's function $\mathbf{G}(\mathbf{r}, \mathbf{r}')$ for the model. If we again use the notation of (4.1), we by (2.5) get

$$\mathbf{G}(\mathbf{r}, \mathbf{r}') = \begin{bmatrix} V(\mathbf{r}, \mathbf{r}', \widehat{\mathbf{e}}_1) \\ V(\mathbf{r}, \mathbf{r}', \widehat{\mathbf{e}}_2) \\ V(\mathbf{r}, \mathbf{r}', \widehat{\mathbf{e}}_3) \end{bmatrix}, \quad |\mathbf{r}| = r_3,\ |\mathbf{r}'| \le r_1, \tag{4.15}$$

where $\widehat{\mathbf{e}}_1$, $\widehat{\mathbf{e}}_2$, $\widehat{\mathbf{e}}_3$ are the unit coordinate vectors.

5 Inverse of dipolar sources in EEG

If we know that the source consists of finitely many dipoles at different points, those dipoles with their locations can be inverted uniquely from a complete,

non-noisy EEG data, at least in principle. Here we shortly discuss how such an inversion can be done by a straightforward least squares search.

Let $\mathbf{Q}_n$ and $\mathbf{p}_n,\ n = 1, \ldots, N$, be the unknown dipoles and their locations, and let $\mathbf{r}_1, \ldots, \mathbf{r}_M \in S$ be the measurement points of the surface potential $V(\mathbf{r}),\ \mathbf{r} \in S$. We assume that $M \geq 6N$. Then

$$V(\mathbf{r}_m) = \sum_{n=1}^{N} \mathbf{G}(\mathbf{r}_m, \mathbf{p}_n) \cdot \mathbf{Q}_n,\ m = 1, \ldots, M. \tag{5.1}$$

We write (5.1) in a matrix form as

$$A(x)\, Q = y \tag{5.2}$$

where $A = A(x)$ is an $M \times 3N$ matrix with rows

$$A(m,:) = [\mathbf{G}(\mathbf{r}_m, \mathbf{p}_1)^T, \ldots, \mathbf{G}(\mathbf{r}_m, \mathbf{p}_N)^T],\ m = 1, \ldots, M, \tag{5.3}$$

x is the $3N \times 1$ column vector of the unknown locations,

$$x = [\mathbf{p}_1; \ldots; \mathbf{p}_N], \tag{5.4}$$

Q is the $3N \times 1$ vector of the unknown dipolar moments,

$$Q = [\mathbf{Q}_1; \ldots; \mathbf{Q}_N], \tag{5.5}$$

and y is the $M \times 1$ vector of the measurements,

$$y = [V(\mathbf{r}_m); \ldots; V(\mathbf{r}_M)]. \tag{5.6}$$

We first solve the overdetermined matrix equation (5.2) for Q and get

$$Q = \Big(A(x)^T A(x)\Big)^{-1} A(x)^T\, y, \tag{5.7}$$

and by substituting that into (5.2) we get a non-linear equation for x as

$$F(x) = 0,\ \text{with } F(x) = \Big(A(x)^T A(x)\Big)^{-1} A(x)^T\, y - y. \tag{5.8}$$

Next (5.8) is solved for x by some appropriate solver of non-linear vector valued equations, like Marquardt's method. After having found y we get Q by (5.7).

Numerical simulations. We ran the search algorithm in the spherical head model in order to find N unknown dipoles, $1 \leq N \leq 10$, both without

and with measurement noise. The number N of dipoles was assumed to be known.

We set N dipoles into random locations into the sphere $|\mathbf{r}| \leq r_1$ with unit moments in random directions. Next we computed the EEG potential $V(\mathbf{r}_m)$ due to the set of these dipoles at the uniformly distributed measurement points $\mathbf{r}_m,\ m = 1, \ldots, M,\ M = 67$ on the upper hemisphere of the sphere $|\mathbf{r}| = r_3$, see Figure (1). We used a random initial guess x_0 for the unknown position vector in the search algorithm.

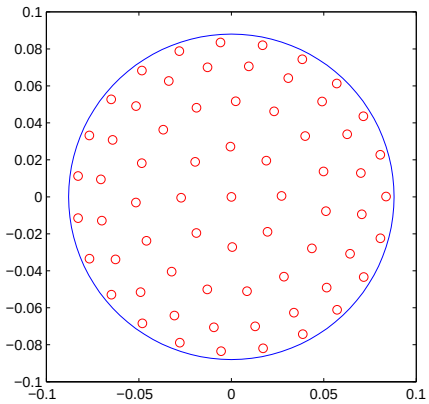

Figure 1: The 67 measurement points on the upper hemisphere seen from above.

First we used noiseless data. The algorithm easily found one dipole. Also two to three dipoles were found but now often a few restarts with new random initial guesses were needed. For $N \geq 4$ the dipoles were not found without restricting random initial guesses. However, using random guesses with distances less than 1 cm from the true positions, the dipoles were found up to $N = 10$.

Next we added $p\,\%$ random noise to the measurement, the percentage taken from the maximal value $V_{max} = \max |\mathrm{V}(\mathbf{r})|$ of the potential (by the MATLAB command: y=y+p/100*V_{max}*randn(size(y));). It turned out that the search algorithm was rather vulnerable to noise with more than one dipole. The algorithm found one dipole for noise $p \leq 10\,\%$, two dipoles for $p \leq 5\,\%$ and three dipoles for $p \leq 2\,\%$. For $N \geq 4$ the dipoles were not found for $p = 1\,\%$. However, using random guesses with distances less than 1 cm from the true positions, the dipoles were found up to $N = 10$ even with $p = 1\,\%$.

6 Inverse of surface sources in EEG

If we know that the current $\mathbf{J}_p$ is distributed on a surface $T \subset D$, we can search for it by expanding it in terms of the so called *lead fields* $\mathbf{L}_m(\mathbf{r}')$, $\mathbf{r}' \in T$, on that surface. The lead fields are simply defined by the Green's function $\mathbf{G}(\mathbf{r}, \mathbf{r}')$ as

$$\mathbf{L}_m(\mathbf{r}') = \mathbf{G}(\mathbf{r}_m, \mathbf{r}'),\ \mathbf{r}' \in T,\ m = 1, \ldots, M, \tag{6.1}$$

wher $\mathbf{r}_1, \ldots, \mathbf{r}_M \in S$ are the measurement points on the boundary S of D. The lead fields play a central role in the inversion problem because

$$V(\mathbf{r}_m) = \int_T \mathbf{G}(\mathbf{r}_m, \mathbf{r}') \cdot \mathbf{J}_p(\mathbf{r}')\, d^2r' \tag{6.2}$$

$$= \int_T \mathbf{L}_m(\mathbf{r}') \cdot \mathbf{J}_p(\mathbf{r}')\, d^2r' = \langle \mathbf{L}_m, \mathbf{J}_p \rangle, \tag{6.3}$$

where we have written the last surface integral over T as the *scalar product*

$$\langle \mathbf{u}, \mathbf{v} \rangle = \int_T \mathbf{u}(\mathbf{r}') \cdot \mathbf{v}(\mathbf{r}')\, d^2r'$$

in the space of all (integrable) vector valued functions $\mathbf{u}$ and $\mathbf{v}$ on T. Equation (6.2) shows that our measurement only sees those sources $\mathbf{J}_p$ which are in the function subspace $\mathcal{L}$ spanned by $\mathbf{L}_1, \ldots, \mathbf{L}_M$, i.e., of the form

$$\mathbf{J}_p = \sum_{n=1}^{M} c_n\, \mathbf{L}_n, \tag{6.4}$$

because the functions $\mathbf{u}$ in the *orthocomplement* of $\mathcal{L}$, i.e., functions $\mathbf{u}$ with $\langle \mathbf{L}_m, \mathbf{u} \rangle = 0,\ m = 1, \ldots, M$, are 'silent' to our measurement $V(\mathbf{r}_1), \ldots, V(\mathbf{r}_M)$. Therefore, it is reasonable to search for $\mathbf{J}_p$ in the form (6.4).

By substituting (6.4) into (6.2) we obtain,

$$V(\mathbf{r}_m) = \langle \mathbf{L}_m, \sum_{n=1}^{M} c_n\, \mathbf{L}_n \rangle,\ m = 1, \ldots, M, \tag{6.5}$$

or in the matrix form

$$A\, c = y \tag{6.6}$$

where

$$A_{m,n} = \langle \mathbf{L}_m, \mathbf{L}_n \rangle = \int_T \mathbf{L}_m(\mathbf{r}') \cdot \mathbf{L}_n(\mathbf{r}')\, d^2r', \tag{6.7}$$

where $1 \leq m, n \leq M,\ c = [c_1, \ldots, c_M]^T$ and $y = [V(\mathbf{r}_1), \ldots, V(\mathbf{r}_M)]^T$.

We solve (6.6) for c and get $\mathbf{J}_p$ as in (6.4). If $\det(A) \neq 0$, the inverse solution $\mathbf{J}_p$ is unique in the subspace $\mathcal{L}$ of 'non-silent' source currents spanned by $\mathbf{L}_1, \ldots, \mathbf{L}_M$. It is not necessarily the true source current $\mathbf{J}_{true}$ but its the *orthogonal projection* of that into $\mathcal{L}$. In that sense $\mathbf{J}_p$ is the *'minimal norm' solution* to the inverse problem, i.e., it solves (6.6) and has the smallest L^2-norm among all the functions $\mathbf{J} \in \mathcal{L}$ which solve (6.6). So, it remains to be seen if $\mathbf{J}_p$ really is equal to $\mathbf{J}_{true}$, or if not, then how much it reveals the characteristic features of the unknown $\mathbf{J}_{true}$.

The good news for EEG is that, if T is a patch of the cortical surface and the $\mathbf{J}_{true}$ is normally directed to T, as it usually is, then the inverted $\mathbf{J}_p$ is a good approximation to $\mathbf{J}_{true}$, in particular, if there are sufficiently many measurement points with low measurement noise.

For the EEG inverse problem we still have to decide how to deal with the measurement noise, i.e., how we solve (6.6), if the measured data in the vector y contains noise. In the next chapter we present one of the elementary methods to cope with noise: the *singular value truncation*.

7 Regularization with the singular value truncation

The *singular value decomposition* (SVD) of an $M \times N$ matrix A is the representation

$$A = U\, D\, V^T \tag{7.1}$$

where U is an $M \times M$ unitary matrix, i.e., $U^T U = I$, V is an $N \times N$ unitary matrix and D is a $M \times N$ diagonal matrix

$$D = \mathrm{diag}\,(\mathrm{d}_1, \ldots, \mathrm{d}_\mathrm{p}),\ \text{with p} = \min(\mathrm{M}, \mathrm{N}), \tag{7.2}$$

where the diagonal elements

$$d_1 \geq \ldots \geq d_r > d_{r+1} = \ldots = d_p = 0, \tag{7.3}$$

are called the *singular values* of A and r =rank(A) is the *rank* of the matrix A (the maximal number of linearly independent column vectors of A). If we write U and V in the terms of their columns,

$$U = [u_1, \ldots, u_M], \;\; V = [v_1, \ldots, v_N], \tag{7.4}$$

we see that $u_1, \ldots, u_M$ form an orthonormal basis of $\mathbb{R}^M$ and $v_1, \ldots, v_N$ an orthonormal basis of $\mathbb{R}^N$, because U and V are unitary.

Consider the equation

$$A\,x = y, \;\; \text{where } \mathrm{x} \in \mathbb{R}^{\mathrm{N}}, \; \mathrm{y} \in \mathbb{R}^{\mathrm{M}}. \tag{7.5}$$

Due to (7.1) and the usual rules of the matrix multiplication we get

$$A\,x = \sum_{n=1}^{r} d_n \langle x, v_n \rangle \, u_n, \tag{7.6}$$

where we denoted the scalar product of column vectors a, $b \in \mathbb{R}^m$ as

$$a \cdot b = a^T\, b = b^T\, a = \langle a, b \rangle. \tag{7.7}$$

For $1 \leq k \leq r$ *the k-truncated SVD solution* of (7.5) is the vector

$$x^{(k)} = \sum_{n=1}^{k} \frac{1}{d_n} \, \langle y, u_n \rangle \, v_n. \tag{7.8}$$

If $k = r = M = N$, it is easy to see, due to (7.6) and the orthonormality of the basis $u_1, \ldots, u_M$ and $v_1, \ldots, v_N$, that $x^{(k)}$ solves (7.5) exactly. Otherwise, by (7.6)

$$A\,x^{(k)} = \sum_{n=1}^{k} \langle y, u_n \rangle \, u_n, \tag{7.9}$$

and so the square of the residual, also called the *discrepancy*, is as

$$\begin{aligned} \delta_k = \left| Ax^{(k)} - y \right|^2 &= \left| \sum_{n=k+1}^{M} \langle y, u_n \rangle u_n \right|^2 \\ &= \sum_{n=k+1}^{M} \langle y, u_n \rangle^2 \end{aligned} \tag{7.10}$$

because y, represented in the orthonormal basis $u_1, \ldots, u_M$, is as

$$y = \sum_{n=1}^{M} \langle y, u_n \rangle \, u_n. \tag{7.11}$$

If $d_n \approx 0$ for $n \geq k+1$, we see by (7.6) that

$$y = Ax \approx \sum_{n=1}^{k} d_n \langle x, v_n \rangle u_n = \sum_{n=1}^{k} \langle y, u_n \rangle u_n, \tag{7.12}$$

and $\left| Ax^{(k)} - y \right| \approx 0$ by (7.10). So, $x^{(k)}$ satisfies (7.5) in this case very well. On the other hand, $x^{(k)}$ is the shortest vector which satisfies

$$Ax = \sum_{n=1}^{k} \langle y, u_n \rangle u_n \tag{7.13}$$

because, if x solves (7.13), then by (7.6) and (7.13)

$$\langle x, v_n \rangle = \frac{1}{d_n} \langle y, u_n \rangle, \ n = 1, \ldots, k, \tag{7.14}$$

and so by (7.8)

$$|x|^2 = \left| x^{(k)} + \sum_{n=k+1}^{N} \langle x, v_n \rangle \, v_n \right|^2 = \left| x^{(k)} \right|^2 + \sum_{n=k+1}^{N} \langle x, v_n \rangle^2 \geq \left| x^{(k)} \right|^2. \tag{7.15}$$

This reasoning tells us that $x^{(k)}$ is a good regularized solution to (7.5) if all d_n are very small for $n \geq k+1$.

Let us next consider (7.5) with noise. Let

$$A \, x_{true} = y_{true}, \tag{7.16}$$

and consider for x the equation

$$A \, x = y, \ \text{ with } \mathrm{y} = \mathrm{y}_{\mathrm{true}} + \mathrm{e} \tag{7.17}$$

with the noise vector $e \in \mathbb{R}^M$. We want to regularize the solution of (7.17) by the SVD truncation by choosing $x^{(k)}$ of (7.8) to be the solution. It remains to decide how to choose the truncation index k to make $x^{(k)}$ a reasonable approximation to the true solution x_{true}. We present here two heuristic methods to choose k.

(Morozov's) Discrepancy Principle. If we (approximately) know $|e|$, it is reasonable to choose k so that

$$\delta_k = \left|Ax^{(k)} - y\right|^2 \approx |e|^2 \tag{7.18}$$

because we know y_{true} only to the accuracy $|y - y_{true}| = |e|$. On the other hand, if we let k increase, we make δ_k possibly much smaller, but at the same time we start increasingly to model the error e in y and possibly increase the error in $x^{(k)}$. So, by the *Discrepancy Principle* we choose k to be the largest k for which

$$\delta_k = \left|Ax^{(k)} - y\right| = \sum_{n=k+1}^{M} \langle y, u_n\rangle^2 \leq |e|^2 . \tag{7.19}$$

The L-curve method. By (7.6) we have

$$y_{true} = A\, x_{true} = \sum_{n=1}^{r} d_n \langle x_{true}, v_n\rangle u_n, \tag{7.20}$$

and so by (7.8) we obtain

$$\left|x^{(k)} - x_{true}\right|^2 = \left|\sum_{n=1}^{k} \frac{1}{d_n}\langle y_{true} + e, u_n\rangle v_n - \sum_{n=1}^{N}\langle x_{true}, v_n\rangle v_n\right| \tag{7.21}$$

$$= \left|\sum_{n=k+1}^{N} \langle x_{true}, v_n\rangle v_n + \sum_{n=1}^{k} \frac{1}{d_n}\langle e, v_n\rangle v_n\right| \tag{7.22}$$

$$= \sum_{n=k+1}^{N} \langle x_{true}, v_n\rangle^2 + \sum_{n=1}^{k} \frac{1}{d_n^2}\langle e, v_n\rangle^2. \tag{7.23}$$

This shows that if d_n become very small as k tends to r, the error in $x^{(k)}$ and also the norm $\left|x^{(k)}\right|$ increase rapidly as k increases toward r. On the other hand, by (7.10) the discrepancy δ_k decreases to

$$\sum_{n=r+1}^{M} \langle y, u_n\rangle^2$$

as k tends to r.

So it is reasonable to let k increase and make δ_k smaller until $\left|x^{(k)}\right|$ starts to grow fast. This point where we should choose $k = k_{trunc}$ often shows in

the L-shaped curve which we obtain by plotting

$$\log \delta_k = \log \Big(\sum_{n=k+1}^{M} \langle y, u_n \rangle^2 \Big) \tag{7.24}$$

as the function of

$$\log \left(\left| x^{(k)} \right|^2 \right) = \log \Big(\sum_{n=1}^{k} \frac{1}{d_n} \langle y, u_n \rangle^2 \Big) \tag{7.25}$$

Then the 'kink' of the L-curve corresponds to the truncation point $k = k_{trunc}$, see Figure (2). However, in practice the L-curve may not resemble the L-shape and so it may be difficult to see where the correct 'kink' is.

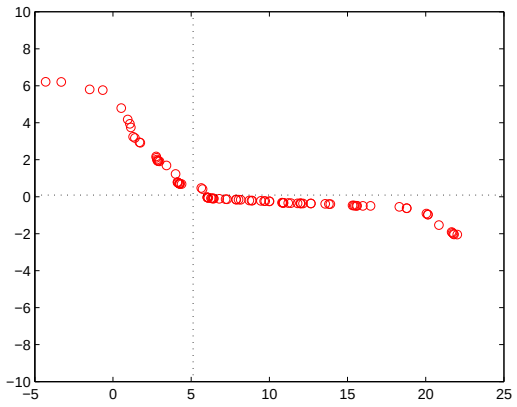

Figure 2: A typical L-curve with a clear kink for determining the truncation point

The Discrepancy Principle is easy to apply in practice, if we really know the size of error vector e, at least approximately. For instance, this is the case if we know that e consists only of the measurement noise and we roughly know that. But if e also contains unknown modeling error, like in using the spherical model for a real head, or the measurement error is unknown, the Principle becomes vague and difficult to apply.

The L-curve method is more robust in the sense that we do not need to know anything about the error vector e. However, if the L-curve does not have the wanted L-shape, also this method becomes vague and difficult to apply.

8 Examples on the inversion of surface current sources in EEG

In the examples here we use the spherically layered sphere (4.12) - (4.14) as the model of the head. The measurement points $\mathbf{r}_1, \ldots, \mathbf{r}_M$ are distributed uniformly over the upper hemisphere $|\mathbf{r}| = r_3$ (the surface of the scalp), with $M = 67$, see Figure (1).

Example 1: *Normally directed source current on the spherical surface* $|\mathbf{r}| = r_1$.

The unknown current $\mathbf{J}_p$ is now of the form

$$\mathbf{J}_p(\mathbf{r}') = J(\mathbf{r}')\,\mathbf{r}'/\,|\mathbf{r}'|\,,\ \text{for}\ |\mathbf{r}'| = r_1, \tag{8.1}$$

where $J(\mathbf{r}'),\ |\mathbf{r}'| = r_1$, is the unknown scalar function. If $\mathbf{G}(\mathbf{r}, \mathbf{r}')$ is the vector Green's function and we use the notation of (4.1), we obtain the potential $V(\mathbf{r}_m)$ at the measurement points as

$$\begin{aligned} V(\mathbf{r}_m) &= \int_{|\mathbf{r}'|=r_1} \mathbf{G}(\mathbf{r}_m, \mathbf{r}') \cdot \mathbf{J}_p(\mathbf{r}')\, d^2r' \\ &= \int_{|\mathbf{r}'|=r_1} V(\mathbf{r}_m, \mathbf{r}', \mathbf{r}'/\,|\mathbf{r}'|)\, J(\mathbf{r}')\, d^2r' \\ &= \int_{|\mathbf{r}'|=r_1} L_m(\mathbf{r}')\, J(\mathbf{r}')\, d^2r', \end{aligned} \tag{8.2}$$

where

$$L_m(\mathbf{r}') = V(\mathbf{r}_m, \mathbf{r}', \mathbf{r}'/\,|\mathbf{r}'|),\ \text{for}\ |\mathbf{r}'| = \mathrm{r}_1,\ \mathrm{m} = 1, \ldots, \mathrm{M}, \tag{8.3}$$

are the *scalar lead fields* assigned to the measurement, see Figure (3). Therefore, we seek for $J(\mathbf{r}')$ in the form

$$J(\mathbf{r}') = \sum_{m=1}^{M} c_m L_m(\mathbf{r}'). \tag{8.4}$$

By inserting this into (8.2), we get the matrix equation

$$A\,c = y \tag{8.5}$$

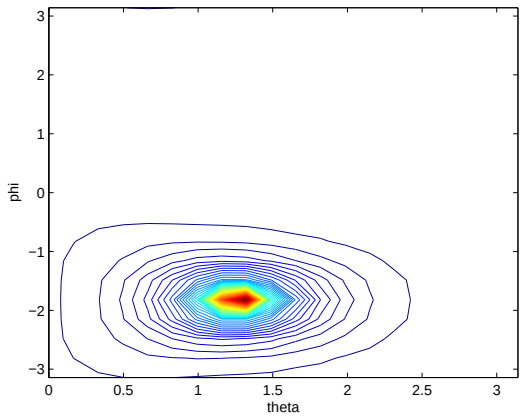

Figure 3: A graph of a typical scalar lead field $L_m(\mathbf{r}')$ on the sphere $|\mathbf{r}'| = r_1$

for the unknown coefficients $c = [c_1, \ldots, c_M]^T$ where

$$A_{m,n} = \int_{|\mathbf{r}'|=r_1} L_m(\mathbf{r}')\, L_n(\mathbf{r}')\, d^2r', \tag{8.6}$$

for $1 \le m, n \le M$, and $y = [V(\mathbf{r}_1), \ldots, V(\mathbf{r}_M)]^T$. We solve (8.5) for c and get J and $\mathbf{J}_p$ as in (8.4) and (8.1).

The integral in (8.6) is over the sphere $|\mathbf{r}| = r_1$, and we use the following integral rule for the numerical integration over a sphere with radius r_1. Let

$$u(\theta, \phi) = L_m(\mathbf{r}')\, L_n(\mathbf{r}') \quad \text{with} \quad \mathbf{r}' = \mathrm{r}_1\, [\sin\theta\, \cos\phi; \sin\theta\, \sin\phi; \cos\theta].$$

Then

$$A_{m,n} = r_1^2 \int_0^{2\pi} \int_0^{\pi} u(\theta, \phi)\, \sin\theta\, d\theta\, d\phi \simeq \sum_{p=1}^{N+1} \sum_{q=0}^{2N} \frac{2\pi\, r_1^2}{2N+1}\, w_p\, u(\theta_p, \phi_q), \tag{8.7}$$

where

$$\theta_p = \arccos(t_p), \quad p = 1, \ldots, N+1, \tag{8.8}$$

$$\phi_q = \frac{2\pi}{2N+1}\, q, \quad q = 0, \ldots, 2N, \tag{8.9}$$

and t_p and w_p are the $N+1$ sampling points and weights of the Gaussian integration rule over the interval $-1 \le t \le 1$. Because the lead fields are very smooth, say $N = 20$, will do in (8.7).

If we take the singular value decomposition of A, we see that A is a regular matrix and the singular values decrease fairly slowly indicating a good resolution in the inverse solution.

Example 2. *Tangentially directed source current on the sphere* $|\mathbf{r}| = r_1$.

here we assume that $\mathbf{J}_p$ is of the form

$$\mathbf{J}_p(\mathbf{r}') = J_\theta(\mathbf{r}')\,\widehat{\theta}(\mathbf{r}') + J_\phi(\mathbf{r}')\,\widehat{\phi}(\mathbf{r}'),\ |\mathbf{r}'| = r_1, \tag{8.10}$$

where $\widehat{\theta}(\mathbf{r}')$ and $\widehat{\phi}(\mathbf{r}')$ are the tangential unit coordinate vectors of the spherical coordinates (r, θ, ϕ),

$$\widehat{\phi}(\mathbf{r}') = [\cos\phi; \sin\phi; 0], \tag{8.11}$$

$$\widehat{\theta}(\mathbf{r}') = \widehat{\phi}(\mathbf{r}') \times \widehat{\mathbf{r}}',\ \ \widehat{\mathbf{r}}' = \mathbf{r}'/\left|\mathbf{r}'\right|, \tag{8.12}$$

where

$$\mathbf{r}' = r_1\,[\sin\theta\cos\phi; \sin\theta\sin\phi; \cos\theta]. \tag{8.13}$$

Now the potential due to $\mathbf{J}_p$ is as

$$\begin{aligned} V(\mathbf{r}_m) &= \int_{|\mathbf{r}'|=r_1} \mathbf{G}(\mathbf{r}, \mathbf{r}') \cdot \mathbf{J}_p(\mathbf{r}')\, d^2r' \\ &= \int_{|\mathbf{r}'|=r_1} \Big(V(\mathbf{r}_m, \mathbf{r}', \widehat{\theta}(\mathbf{r}'))\, J_\theta(\mathbf{r}') + V(\mathbf{r}_m, \mathbf{r}', \widehat{\phi}(\mathbf{r}'))\, J_\phi(\mathbf{r}') \Big)\, d^2r' \\ &= \int_{|\mathbf{r}'|=r_1} \mathbf{L}_m(\mathbf{r}') \cdot \mathbf{J}_p(\mathbf{r}')\, d^2r' \end{aligned} \tag{8.14}$$

with the *vector lead fields*

$$\mathbf{L}_m(\mathbf{r}') = V(\mathbf{r}_m, \mathbf{r}', \widehat{\theta}(\mathbf{r}'))\,\widehat{\theta}(\mathbf{r}') + V(\mathbf{r}_m, \mathbf{r}', \widehat{\phi}(\mathbf{r}'))\,\widehat{\phi}(\mathbf{r}'). \tag{8.15}$$

Accordingly, we seek for $\mathbf{J}_p$ in the form

$$\mathbf{J}_p(\mathbf{r}') = \sum_{m=1}^{M} c_m\, \mathbf{L}_m(\mathbf{r}') \tag{8.16}$$

and get for $c = [c_1, \ldots, c_M]^T$ the equation

$$A\,c = [V(\mathbf{r}_1), \ldots, V(\mathbf{r}_M)]^T \tag{8.17}$$

with

$$A_{m,n} = \int_{|\mathbf{r}'|=r_1} \mathbf{L}_m(\mathbf{r}') \cdot \mathbf{L}_n(\mathbf{r}')\, d^2r'. \tag{8.18}$$

After having solved (8.17) for c we get $\mathbf{J}_p$ as in (8.16).

Example 3. *Source current* $\mathbf{J}_p$ *on the sphere* $|\mathbf{r}'| = r_1$ *with free direction of* $\mathbf{J}_p/\,|\mathbf{J}_p|$.

This is just the case in Chapter 6 with the surface T being the sphere $|\mathbf{r}'| = r_1$.

Numerical simulations. We first examine how well our inversion method finds a single dipole on the sphere $|\mathbf{r}'| = r_1$.

We start by setting a normally directed unit dipole at an arbitrary location on the sphere $|\mathbf{r}'| = r_1$, compute the potentials $V(\mathbf{r}_m),\ m = 1, \ldots, M$, and solve (8.5) for a normally directed $\mathbf{J}_p$. The level curves of $|\mathbf{J}_p|$ are presented in Figure (4) with the location of the source dipole marked with a circle. We see that the level curve pattern of $|\mathbf{J}_p|$ shows the location rather well.

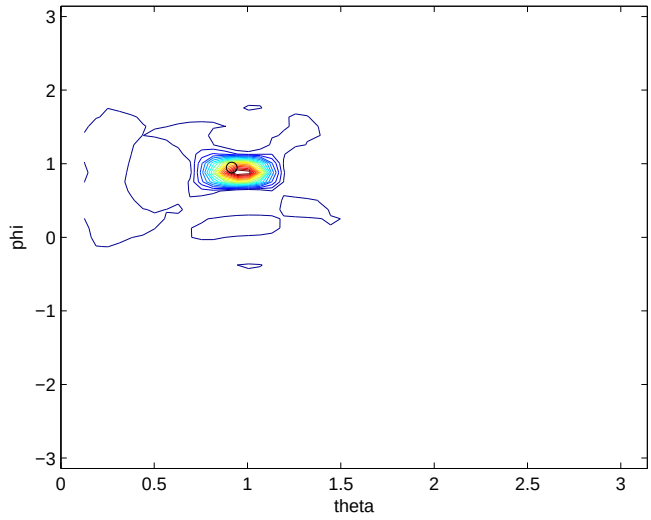

Figure 4: The level curves of $|\mathbf{J}_p|$ where $\mathbf{J}_p$ is normally directed and the true source is a normally directed dipole whose location is marked with a circle.

Next we repeat the same experiment so that both $\mathbf{J}_p$ and the source

dipole are tangentially directed. The result is shown in Figure (5), where $\mathbf{J}_p$ is depicted with arrows and $|\mathbf{J}_p|$ with level curves. In fact, it can be shown that the inverted $\mathbf{J}_p$ is not equal to the true source dipole $\mathbf{J}_{true}$ but presents the irrotational part of $\mathbf{J}_{true}$ in the Helmholtz decomposition of $\mathbf{J}_{true}$ into the solenoidal and irrotational parts. This can be seen in Figure (5) $\mathbf{J}_p$ presenting the 'return' currents. However, the level curve pattern rather well shows the location of the true source.

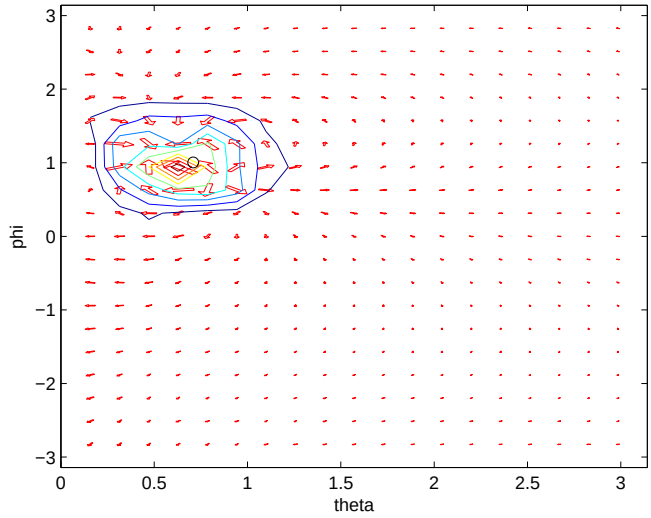

Figure 5: The arrow field of $\mathbf{J}_p$ and the level curves of $|\mathbf{J}_p|$ where $\mathbf{J}_p$ and the source dipole are tangentially directed. The location of the source dipole is marked with a circle.

Next we study how well a source of three dipoles at arbitrary locations on the sphere $|\mathbf{r}'| = r_1$ can be recovered by $\mathbf{J}_p$.

First we let the dipoles and $\mathbf{J}_p$ be normally directed and add 10% non-correlated noise to the measurements, the percentage taken from the maximum of the measured potential. The solution is regularized by the Discrepancy Principle. The resulting $|\mathbf{J}_p|$ is shown in Figure (6). Again, the level curve pattern fairly well shows the locations of the source dipoles.

Next the same experiment is repeated for tangentially directed 3 source dipoles and $\mathbf{J}_p$ and with 10% noise. The solution is regularized by the Discrepancy Principle. The results are shown in Figure (7). The level curve pattern of $|\mathbf{J}_p|$ is somewhat more spread but again it shows rather well the

locations of the source dipoles.

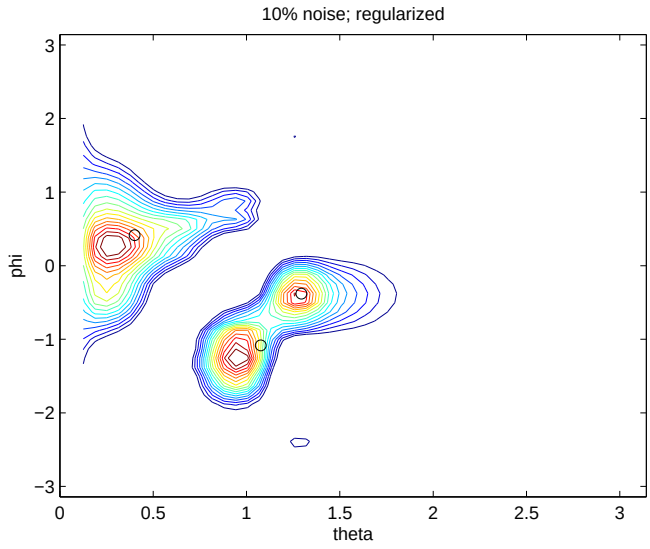

Figure 6: Level curves of $|\mathbf{J}_p|$ where $\mathbf{J}_p$ and the 3 source dipoles (locations marked with circles) are normally directed.

In the next experiment we put the source dipoles 1 cm below the surface $|\mathbf{r}| = r_1$ where $\mathbf{J}_p$ is residing. So we search for *an equivalent source current* $\mathbf{J}_p$ yielding the same measured potential as the true source.

The source dipoles have arbitrarily directed unit moments $\mathbf{Q}$. We added 5% noise to the measurements and solved for three types of $\mathbf{J}_p$: normally, tangentially and freely directed. The solutions were regularized by the Discrepancy Principle. The results are shown in Figure (8). We see that the freely oriented $\mathbf{J}_p$ best shows the locations of the source dipoles.

In the Figure (9) the same experiment with 5 dipoles is repeated. Again the freely oriented $\mathbf{J}_p$ seems to show the true positions best.

Example 3. In this example we search for the currents $\mathbf{J}_p$ on a rectangular plate T in the yz-plane depicted in Figure (10). We let $\mathbf{J}_p$ be normally, tangentially and freely directed. The corresponding lead fields are found as in the Examples 1 and 2 by using the two orthogonal unit vectors $\widehat{\mathbf{u}}$ and $\widehat{\mathbf{v}}$ which span the plane of T. We choose three source dipoles at arbitrary locations on T and compute the measurements, and thereafter, we search for the solution $\mathbf{J}_p$ on T.

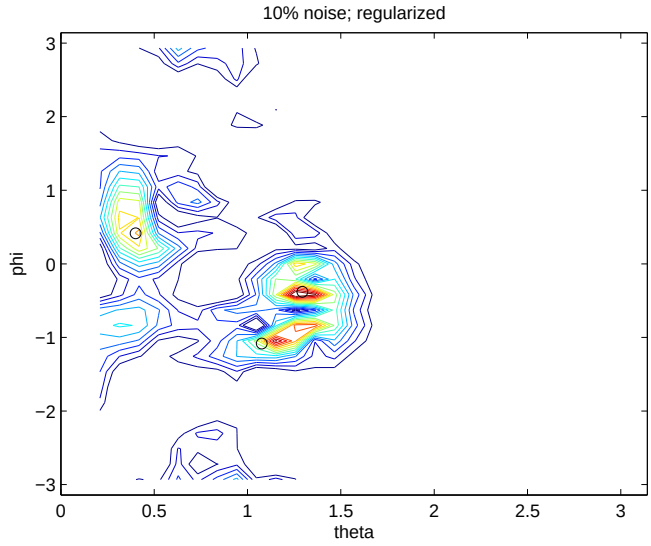

Figure 7: Level curves of $|\mathbf{J}_p|$ where $\mathbf{J}_p$ and the 3 source dipoles (locations marked with circles) are tangentially directed.

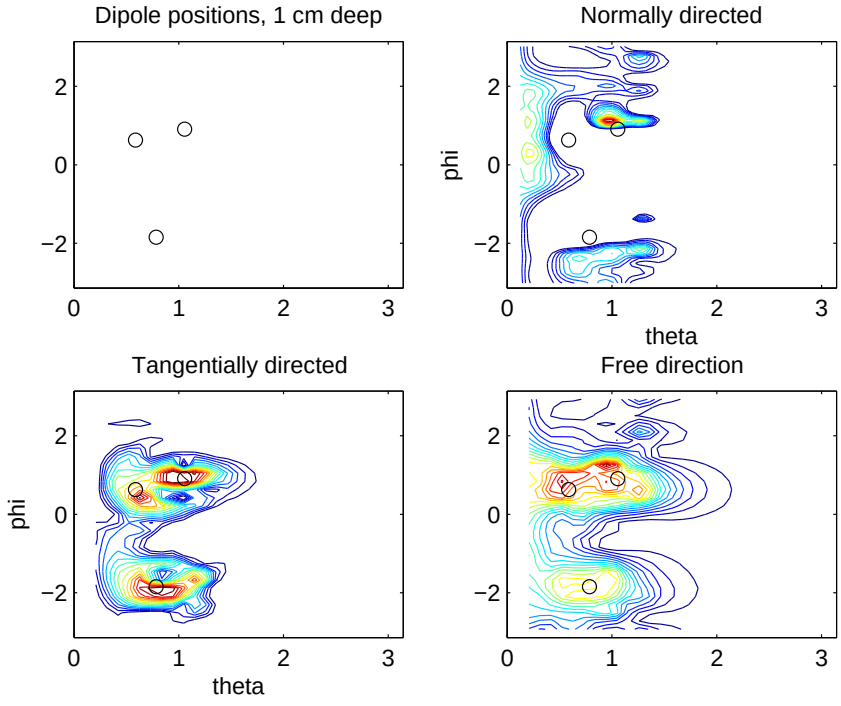

Figure 8: Level curves of normally, tangentially and freely directed equivalent currents $\mathbf{J}_p$

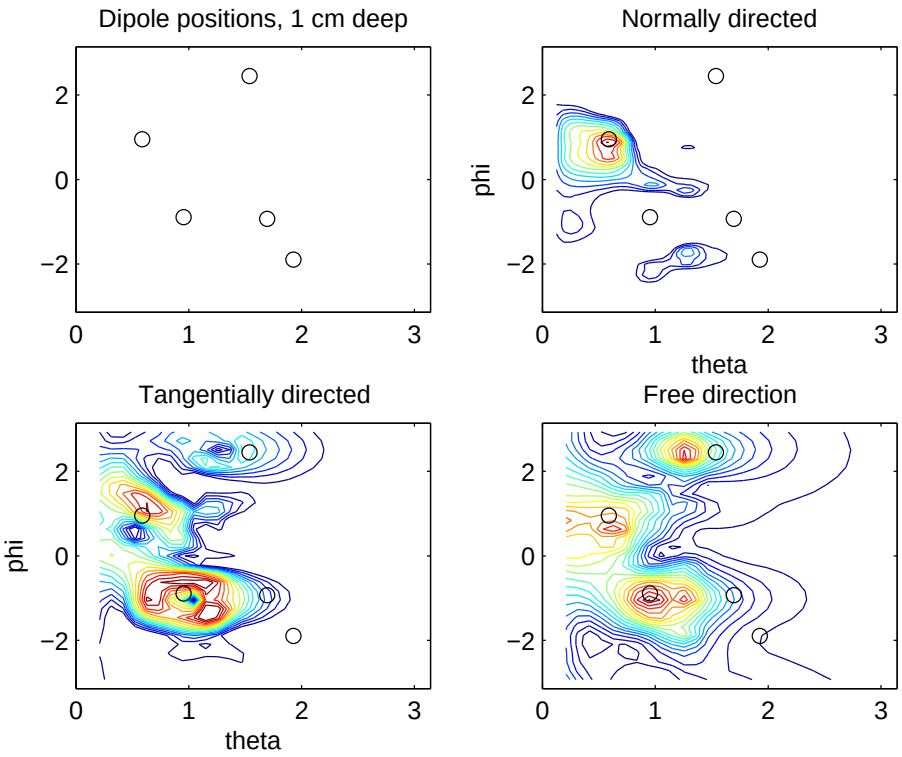

Figure 9: Locations of 5 dipoles and level curves of normally, tangentially and freely directed equivalent currents $\mathbf{J}_p$

First we let the dipoles and $\mathbf{J}_p$ be normally or tangentially directed. We must add slightly noise ($10^{-6}\%$) to the measurements and regularize by the Dicrepancy Principle in order to remove the bad ill-poisedness of the matrix A. The results are shown in Figures (11) and (12). We see that the normally directed $\mathbf{J}_p$ slightly better shows the positions of the dipoles.

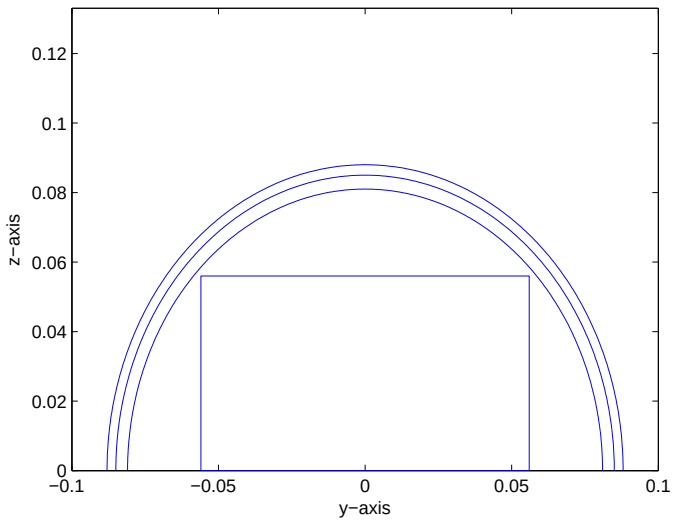

Figure 10: Rectangular plate in the yz-plane in the upper hemisphere of the spherical head model.

In the last experiment we let the 3 source dipoles be arbitrarily directed. We add 1% noise to the measurements and use the Discrepancy Principle for regularization. We let $\mathbf{J}_p$ be either normally, tangentially or freely directed. The somewhat surprising results are shown in Figure (13). The normally and tangentially directed $\mathbf{J}_p$ cannot at all find the true sources while the freely directed $\mathbf{J}_p$ manages much better. Note that the upright plate extending down to the center of the spherical model leads anyway to a rather ill-posed EEG inverse problem.

This example suggests that the normally and tangentially directed $\mathbf{J}_p$ are not good choices for an inverse candidate on a patch of surface if the direction of the true source current is not rather accurately known.

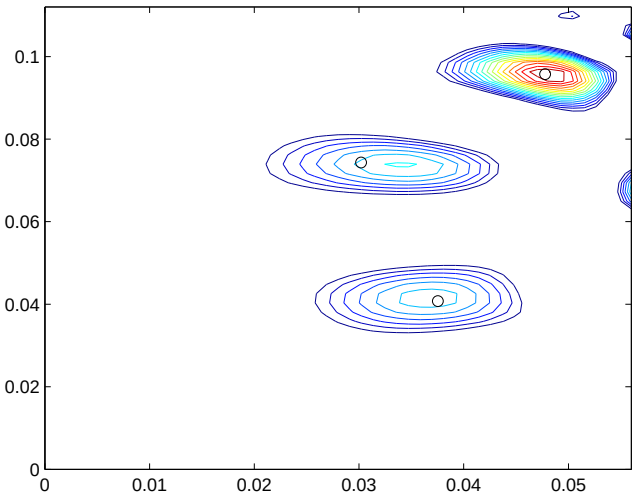

Figure 11: Level curves of the normally directed $\mathbf{J}_p$ on the rectangular plate T.

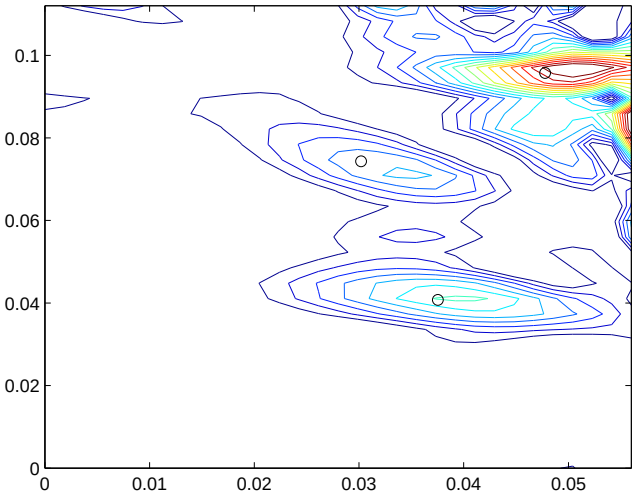

Figure 12: Level curves of the tangentially directed $\mathbf{J}_p$ on the rectangular plate T.

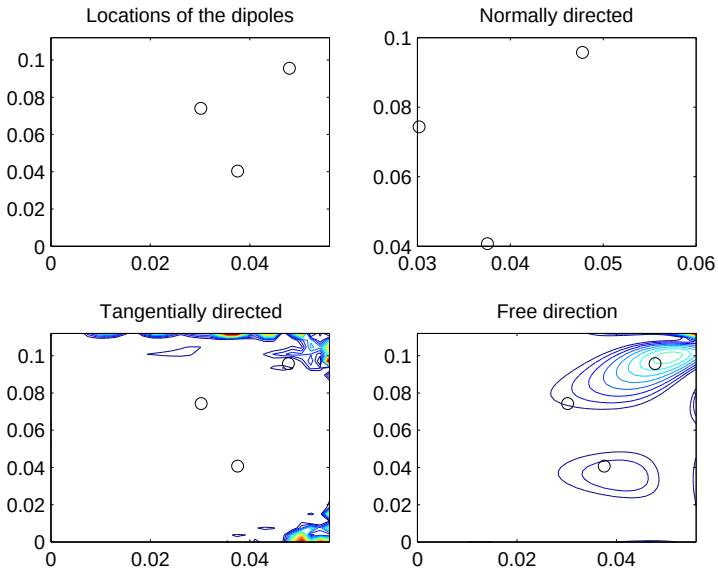

Figure 13: Level curves of the normally, tangentially and freely directed $\mathbf{J}_p$ on the plate T with 3 arbitrarily directed source dipoles.

References

[1] Kaipio, J. P and Somersalo,E, *Statistical and Computational Inverse problems*, Springer-Verlag, Berlin, Heidelberg, New York 2005,

[2] Mosher, C., Leahy, M. and Lewis, P., *EEG and MEG: Forward Solutions for Inverse Methods*, IEEE Transactions on Biomedical Engineering, VOL. 46, NO. 3, March 1999.